**CHAPTER 7**

# Simulations of Arctic Mixed-Phase Boundary Layer Clouds: Advances in Understanding and Outstanding Questions

**Ann M. Fridlind, Andrew S. Ackerman**
National Aeronautics and Space Administration, Goddard Institute for Space Studies, New York, NY, United States

## Contents

## 1. INTRODUCTION

The objective of this chapter is to provide an overview of mixed–phase boundary layer cloud simulations. Our emphasis is on what detailed studies show—in particular what is

not relatively well understood or observed about the microphysical processes within such clouds—using analogous liquid-phase boundary layer clouds as a reference for the dynamical conditions. Since boundary layer clouds are characterized by turbulent mixing, the large-eddy simulation (LES) approach has been most widely used to represent the coupling between dynamical and mixed-phase microphysical processes, although there are limits to its ability to represent cloud-top entrainment and associated microphysical details at cloud top (e.g., Klingebiel et al., 2015; Mellado, 2016). Nevertheless, many LES studies of mixed-phase boundary layer clouds have been made over the past 20 years that the LES approach has been a relatively widely used technique. Among these are several model intercomparison studies that include results from differing LES models simulating the same case study.

Thus far nearly all detailed LES and intercomparison studies have been based on specific cloud systems observed during field campaigns. Whereas other chapters of this book broadly summarize observational findings, here we focus primarily on modeling results from three major field campaigns on which intercomparison studies have been based: the First International Satellite Cloud Climatology Project (ISCCP) Regional Experiment-Arctic Cloud Experiment (FIRE-ACE)/Surface Heat Budget in the Arctic (SHEBA) campaign (SHEBA; Curry et al., 2000), the Mixed-Phase Arctic Cloud Experiment (M-PACE; Verlinde et al., 2007), and the Indirect and Semi-Direct Aerosol Campaign (ISDAC; McFarquhar et al., 2011). Table 1 summarizes the general cloud-system properties for the respective intercomparison case studies based on observations from SHEBA (Morrison et al., 2011), M-PACE (Klein et al., 2009), and ISDAC (Ovchinnikov et al., 2014). Fig. 1 shows a satellite image representative of each case.

The case studies in Table 1 span a range of liquid water path (LWP), aerosol loading, and cloud temperatures. Considering the case studies as liquid-phase only for a moment and placing them in the context of LWP and droplet number concentration ($N_d$), they can be seen to span conditions from very thin, polluted clouds in the SHEBA case to very thick, clean clouds in the M-PACE case (Fig. 2). Drizzle can be expected to be an active process in liquid-phase clouds where $LWP/N_d \gg 0.1$ g m$^{-2}$ cm$^3$ (Comstock et al., 2004), as in the M-PACE case. Drizzle drops are conspicuous in Cloud Particle Imager (CPI) data for that

**Table 1** Mixed-phase boundary layer cloud model intercomparison case studies

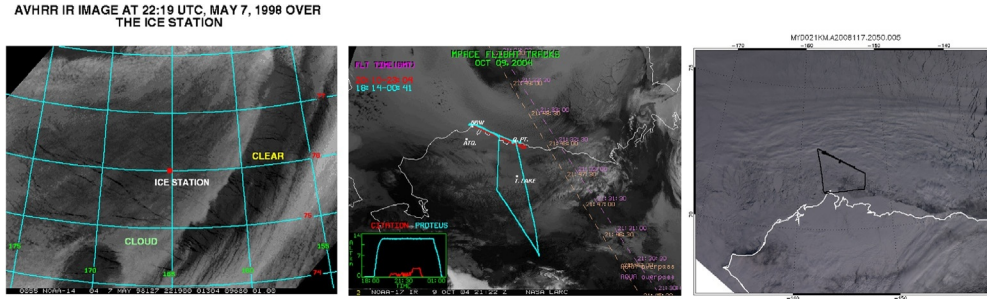| Field campaign | Observation period (UTC) | Cloud top height (m) | Cloud temp. (°C) Top | Base | Path (g m$^{-2}$) Liquid | Ice | Conc. (cm$^{-3}$) Drops | Ice |
|---|---|---|---|---|---|---|---|---|
| SHEBA | May 7, 1998 | 500 | −20 | −18 | 5–20 | 0.2–1 | 200 | ∼0.0001 |
| M-PACE | Oct. 9–10, 2004 | 1000 | −16 | −9 | 110–210 | 8–30 | 40 | ∼0.01 |
| ISDAC | Apr. 26, 2008 | 800 | −15 | −11 | 10–40 | 2–6 | 200 | ∼0.001 |

**Fig. 1** Observation period satellite imagery from SHEBA (infrared; left; May 7 sea ice station location shown), M-PACE (infrared; middle; flight 9a track from Barrow, Alaska to Oliktok Point shown along coast), and ISDAC (mid-visible; right; flight 31 track from Barrow shown).
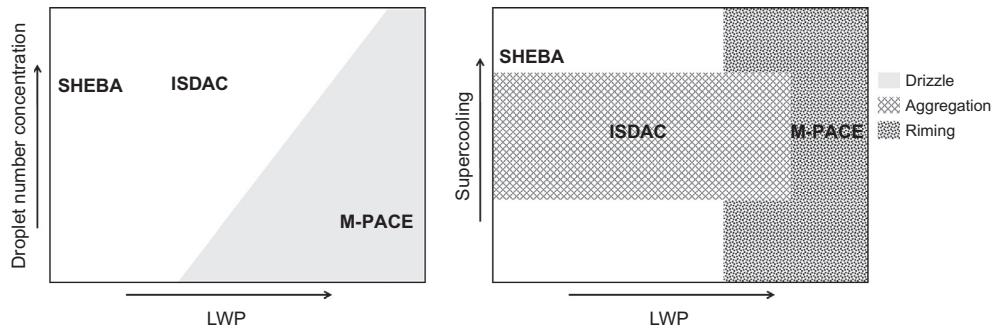


**Fig. 2** Model intercomparison case studies ranked by liquid-phase (left) and ice-phase (right) cloud microphysical processes.

case, consistent with past evidence of drizzle formation under supercooled conditions (e.g., Cober et al., 1996). Drizzle in mixed-phase clouds is discussed further below.

Perhaps less easily deduced from the values listed in Table 1 are active ice-phase cloud microphysical processes. By definition all mixed-phase clouds contain ice crystals, which are formed evidently in part via heterogeneous nucleation (as discussed further below), and they grow most rapidly via vapor diffusion within the cloud layer, where humidity is saturated with respect to liquid and correspondingly supersaturated with respect to ice. As long as liquid cloud base is supercooled, as in all cases in Table 1, ice-supersaturated conditions extend below liquid cloud base. A deep layer of the cloud-topped boundary layer that extends from cloud top to below supercooled cloud base is thus a region where diffusional growth of ice is active. Ice throughout that zone is growing in both updrafts and downdrafts, both above and below cloud base.

Analogous to drizzle formation via a warm-phase collision–coalescence process, riming and ice aggregation may also be expected active ice growth processes via mixed-phase

and ice–ice collection. Placing case studies in the context of LWP and supercooling, riming can be roughly understood to accompany high LWP (Fig. 2), although it should be noted that observations indicate that a mean droplet diameter of 10 µm is also required for the process to be an efficient growth mechanism (e.g., Lowenthal et al., 2011). Aggregation, on the other hand, may conceivably be roughly understood to accompany the presence of sufficiently numerous dendritic particles to undergo entanglement (e.g., Mitchell, 1988, and references contained therein). We represent this in Fig. 2 as a range of cloud supercooling around −15°C with a high LWP limit above which active riming may largely eliminate dendrites, as observed in the M-PACE case. At colder temperatures, the dendritic growth habit is not favored (e.g., Pruppacher and Klett, 1997), as consistent with observations from the SHEBA case study.

Taking the liquid- and ice-phase process occurrences in Fig. 2 together, SHEBA can be identified as the simplest case study insofar as no collisional processes are active. In the ISDAC case, aggregation is active. In the M-PACE case, drizzle and riming are active. For the purposes of illustrating model representation of these processes, we will discuss the case studies below in order of increasing complexity, drawing on related studies that accompany each intercomparison work. We then discuss open questions common to all case studies, and avenues for future progress.

## 2. SHEBA CASE STUDY

The conditions observed on May 7, 1998 over the SHEBA sea ice camp at roughly 76°N, 165°W occurred within a nine-day period dominated by shallow mixed-phase cloud over pack ice with a variable cloud-top height of 400–1200 m and LWP commonly exceeding $20 \, \mathrm{g \, m^{-2}}$ (Zuidema et al., 2005). The 12-h period selected for the Morrison et al. (2011) model intercomparison study, 12–24 UTC, exhibited weak winds of roughly $5 \, \mathrm{m \, s^{-1}}$ within a shallow cloud-topped boundary layer that was relatively well-mixed from surface to cloud top. Sustained radar reflectivity at all elevations below cloud top indicates persistent, continuous mixed-phase conditions (Fig. 3).

A notable feature of the SHEBA case study relative to others is that boundary layer air is supersaturated with respect to ice from cloud top (where liquid saturation defines substantial ice supersaturation) down to the surface, indicating that ice sublimation is not an active process (cf. Morrison et al., 2011, their Fig. 9a). This leaves three active liquid-phase processes (droplet activation, primarily within updrafts at cloud base; droplet growth, primarily within updrafts above cloud base; and droplet evaporation, primarily within downdrafts above cloud base) and two active ice-phase processes (ice nucleation, likely somewhere within the liquid-phase region; and ice diffusional growth, at all elevations throughout the cloud-topped turbulent boundary layer).
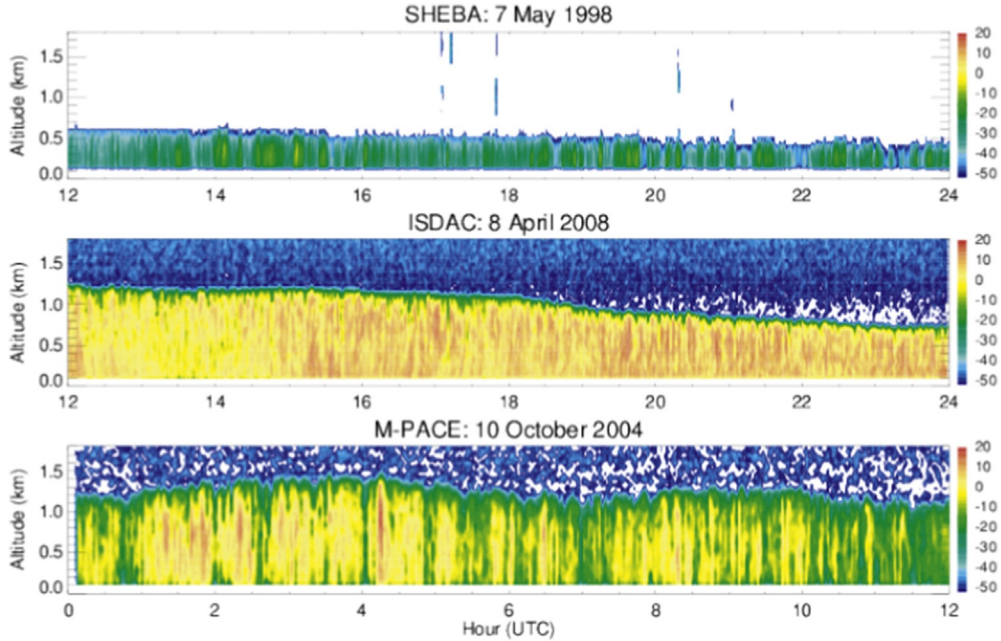
**Fig. 3** Vertically pointing millimeter-wavelength cloud radar (MMCR) reflectivity (dBZ) observations during 12-h periods representative of the SHEBA, ISDAC, and M-PACE case studies.

## 2.1 Ice Crystal Number Concentration Budget

Fig. 4 illustrates the steady–state budget for ice crystal number concentration within a well–mixed boundary layer with steady cloud-top height and temperature in the case that ice crystals are formed exclusively via the activation of aerosol ice-freezing nuclei[1](IFN) that are entrained from the overlying free troposphere and rapidly nucleated, as commonly assumed (e.g., Pinto, 1998; Harrington and Olsson, 2001). Fig. 4 illustrates the steady-state budget for ice crystal number concentration within a well-mixed boundary layer with steady cloud-top height and temperature. Horizontal flux divergences are neglected. The only supply of new ice crystals to the boundary layer is via entrainment of heterogeneous ice-freezing nuclei at cloud top, which depends upon cloud-top entrainment rate ($w_e$). In the absence of aggregation and sublimation, the only sink of crystals is sedimentation to the surface, which can be cast in terms of number-weighted ice crystal fall speed ($v_f$). LES and observations both support approximating ice particle size distributions (PSDs) as vertically uniform in a well-mixed boundary layer (e.g., Fridlind et al., 2007; McFarquhar et al., 2007, 2011; Fridlind et al., 2012).

---

[1] Owing to lack of ambiguities that could occur in some literature (e.g., Vali et al., 2015), here we follow the traditional Pruppacher and Klett (1997) terminology for IFN, which parallels terminology for cloud condensation nuclei (CCN) in cloud microphysics literature.
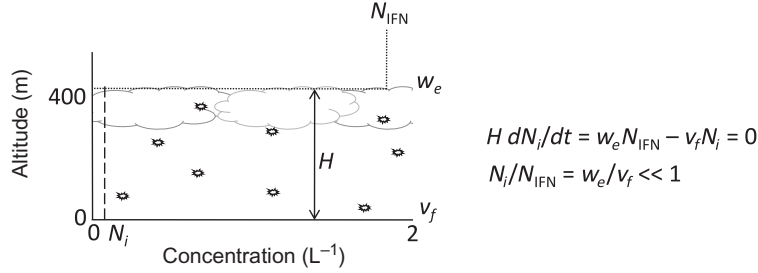
**Fig. 4** Steady-state budget for ice crystal number concentration ($N_i$) in the SHEBA case, where $H$ is boundary layer height, $N_{IFN}$ is overlying ice nucleus number concentration, $w_e$ of $\sim$0.1 cm s$^{-1}$ is cloud-top entrainment rate, and $v_f$ of $\sim$30 cm s$^{-1}$ is number-weighted ice crystal fall speed at the surface, following Fridlind et al. (2012).

The salient result of the mixed–layer budget (cf. Fridlind et al., 2012) is that the ice crystal number concentration within the boundary layer ($N_i$) is found to be proportional to the product of the overlying IFN number concentration ($N_{IFN}$) and the ratio of cloud–top entrainment rate to the number-weighted ice crystal number concentration ($w_e/v_f$). Given LES estimates of $v_f$ circa 30 cm s$^{-1}$ and $w_e$ c.0.1 cm s$^{-1}$, $N_i$ is then two orders of magnitude smaller than $N_{IFN}$, which presents a stark contrast to $N_i \approx N_{IFN}$ near the leading edge of an orographic wave cloud (Eidhammer et al., 2010), for instance, where entrainment does not present a limitation to the supply of IFN.

Budgets based on LES of the SHEBA case study support this key result that $N_i \ll N_{IFN}$ under the assumptions just stated (Fridlind et al., 2012). The simulations also yield an ice crystal lifetime within the well–mixed boundary layer of roughly 1 h in this case, consistent with estimates obtained by other means for the ISDAC case study (Yang et al., 2013). Here we have assumed that all IFN are those that will activate essentially instantaneously in a measurable mode under cloud-top conditions, which are the coldest and most supersaturated within the boundary layer. LES results are insensitive to whether the IFN nucleation mode is assumed to be condensation, immersion, or deposition, but contact–mode nucleation is found to be in a separate class wherein the rate of collection of IFN by supercooled droplets does not yield rapid activation (Fridlind et al., 2012), consistent with assumptions that measurements made by a Counter–Flow Diffusion Chamber (CFDC; Rogers et al., 2001) instrument under cloud-top conditions do not include contact nucleation. Because the role of contact–mode nucleation remains uncertain (e.g., Ladino Moreno et al., 2013) we will return to this point later.

## 2.2 Intercomparison Specification

Model intercomparison studies commonly make a number of simplifying assumptions to limit the model components being tested and thereby the chances of being overwhelmed

by diversity of model behaviors. For instance, surface turbulent heat fluxes may be spec-
ified and radiative transfer replaced with a simple parameterization (e.g., Ovchinnikov
et al., 2014). In the case of the SHEBA model intercomparison, ice nucleation was also
specified with a simple parameterization that maintains $N_i$ approximately fixed at 1.7 $L^{-1}$
(referred to as BASE), with sensitivity tests using 0.17 $L^{-1}$ (LOWNI) and 5.1 $L^{-1}$
(HIGHNI). The BASE value was selected to give $N_i$ equal to the overlying $N_{IFN}$ (at
cloud-top temperature) based on observational evidence of approximate equivalence
reported in field measurements (Prenni et al., 2009), in contrast to the budget argument
provided above.

Large-scale subsidence and advective tendencies of heat and moisture must be applied
to LES with periodic boundary conditions considered in an Eulerian rather than Lagrang-
ian column framework, but such forcings are poorly constrained (e.g., Jiang et al., 2000;
Morrison and Pinto, 2004). It is the rule rather than the exception that they are selected to
produce observed conditions at least to some degree, as discussed by Vogelmann et al.
(2015), who demonstrate the diversity of shallow cloud simulations that can result when
large-scale forcings are adopted wholesale from a range of potential sources (global or
regional reanalyses or mesoscale model simulations). In the case of the SHEBA case study
specification, with $N_i$ fixed at 1.7 $L^{-1}$, the large-scale forcings are selected to maintain
LWP, cloud-top height, and thermodynamic profiles in quasi-equilibrium over the
12-h simulation time (cf. Morrison et al., 2011, their Fig. 4). If LOWNI or HIGHNI
were adopted as the baseline, large-scale forcings would be selected to account for a lesser
or greater desiccation rate. This relationship between specified large-scale forcings and
specified $N_i$ in sustaining a shallow mixed-phase cloud was well demonstrated by
Jiang et al. (2000).

## 2.3 Intercomparison Results

It is seen in the intercomparison study that two-thirds of LES models maintain LWP in a
quasi-steady state in the BASE case, as intended (cf. Morrison et al., 2011, their Fig. 4).
The LOWNI case is reported to be similar to an ice-free state, and all models produce
greater LWP by varying amounts. In the HIGHNI case, most models cannot maintain
steady LWP. Using the estimates of $w_e$ and $N_{IFN}$ listed above, the HIGHNI case would
correspond to a free troposphere concentration of rapidly nucleated IFN of $\sim 1500 \, L^{-1}$,
which exceeds by roughly an order of magnitude those reported at any temperature in
commonly used compilations of CFDC measurements (cf. DeMott et al., 2010).

Given extreme uncertainty in the actual concentration of ice based on in situ mea-
surements within mixed-phase clouds (e.g., Fridlind et al., 2007, factor of 5) and the like-
lihood that unknown secondary ice multiplication mechanisms may exist with poorly
defined limits (e.g., Yano and Phillips, 2011; Ackerman et al., 2015; Lawson et al.,

2015), it is vital to know quantitatively what ice loadings occur under commonly observed conditions. In their intercomparison case study Morrison et al. (2011) highlight the capability of high $N_i$ to lead to complete cloud glaciation.

## 2.4 Additional Observational Constraints

Using the intercomparison case study as a foundation, Fridlind et al. (2012) sought additional constraints on ice loading by making two additional comparisons between the BASE simulation and observations. First, they compared radar reflectivity ($Z$) and mean Doppler velocity ($V_D$) measured by a Millimeter-wavelength Cloud Radar (MMCR) at the sea ice camp with that forward-simulated from the LES. Second, they compared in situ aircraft measurements of ice PSDs made below liquid cloud base, where conditions are relatively uniform with height, with those simulated. The last 2 h of the 12-h intercomparison period were selected to bound the aircraft sampling period.

Fridlind et al. (2012) found that their BASE intercomparison simulation overestimated median $Z$ by roughly 12 dBZ, but quite accurately represented median $V_D$, indicating that ice PSDs were quite consistent with remote-sensing measurements but $N_i$ was too great, all else being equal. Adjusting the case study specification, especially reducing both $N_i$ and large-scale moisture convergence and increasing heat divergence, served to bring the LES results into line with both radar and in situ measurements simultaneously. The resulting simulation yielded a weak desiccation rate with $N_i$ of circa 0.3 L$^{-1}$, allowing mixed-phase persistence over a 4-h simulation despite LWP of only 5 g m$^{-2}$. Weak desiccation can be considered as qualitatively consistent with the prevalence of long-lived mixed-phase conditions in observations (e.g., Shupe et al., 2006).

However, Fridlind et al. (2012) also found that a rapidly-nucleated overlying IFN concentration of roughly 50 L$^{-1}$ would be required to explain in situ and radar observations of ice properties. At a cloud-top temperature of $-20°$C, this is still a very high concentration relative to global CFDC measurements (cf. DeMott et al., 2010). The occurrence of persistent ice precipitation from mixed-phase layer clouds that may not be greatly desiccating but still greatly exceeds the effect of observationally supported $N_{IFN}$ values has been reported elsewhere (Westbrook and Illingworth, 2013), as discussed further below. Fridlind et al. (2012) also conclude that simulations are sensitive to the ice crystal physical properties that determine fall speed and growth rate, which are not quantitatively constrained by existing observational analyses. Thus while radar and in situ measurements provide constraints on obtaining a relatively realistic mixed-phase cloud state that is consistent with observations in many ways, two factors remained exceptionally poorly constrained: the mechanism(s) of new ice crystal formation and the ice crystal physical properties (see Fig. 5).
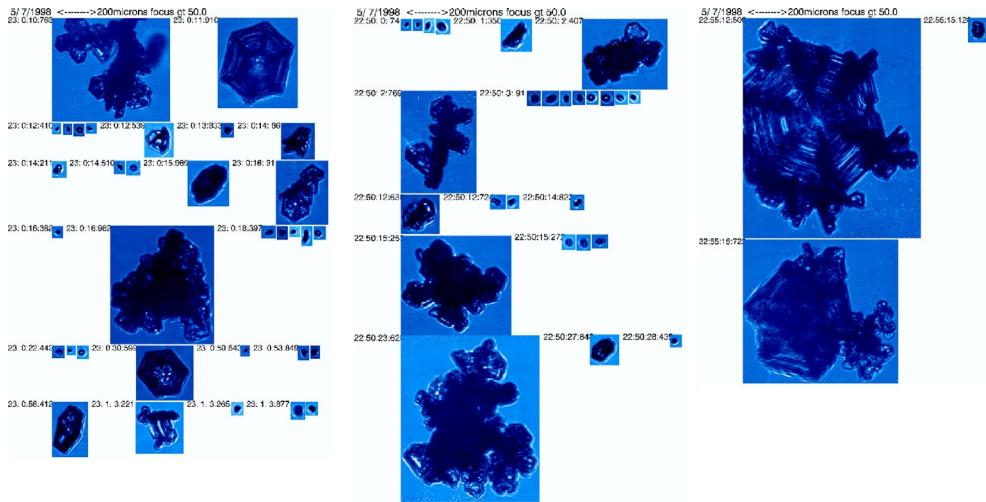
**Fig. 5** Cloud Particle Imager (CPI) data collected on the C-130 aircraft during the SHEBA case study observation period show a variety of radiating plate shapes.

## 2.5 SHEBA Lessons

For the purposes of understanding the fundamentals of mixed-phase boundary layer clouds, the SHEBA case study has demonstrated that mixed-phase clouds can be very simple. In this case: a non-drizzling warm-phase stratocumulus type cloud plus the weak production of ice crystals that grow by vapor diffusion within the turbulent boundary layer until they sediment out. It is intuitive to consider the ice-free state and addition of a scarcely perceptible amount of ice, which is not dissimilar to observer experiences reported for this case study. If each crystal experiences the cloud conditions independently and LWP is unaffected, a characteristic ice size distribution can be considered to emerge from the results of crystals growing and sedimenting within a turbulent layer. If twice as many ice crystals are nucleated (anywhere in the cloud, it turns out), the horizontal-mean ice PSDs are shifted directly upward and the distribution of $V_D$ is unaffected, as found in LES results (Fridlind et al., 2012). As more and more ice crystals are added, LWP will eventually be reduced and total desiccation could proceed as found for the Morrison et al. (2011) HIGHNI case.

It is notable that desiccation appears weak in the constrained case study of Fridlind et al. (2012). However, it is also notable that ice nucleation appears substantially stronger than would be expected from in situ measurements of overlying IFN during the case study (roughly 30 times greater) or globally. Fridlind et al. (2012) discuss conceivable causes for this, such as blowing snow despite weak winds. As shown further below, a lack

of adequate IFN to explain observed ice appears to be the rule rather than exception in observed case studies for as yet undetermined reasons.

LES with broadly accepted (hereafter "known") physics are consistent with the observed coexistence of liquid and ice, and can reproduce close simulacra of observed conditions on many counts simultaneously. Degree of success depends on tuning ice production rate upwards in this case and probably also depends in part on tuning large-scale forcing terms, which could mask simulation errors, such as in cloud-top entrainment rate or ice crystal vapor growth rate. Requiring a model with relatively few internal tuning knobs to reproduce many observations at once within observationally determined uncertainties nonetheless provides some degree of a test of known physics. Within uncertainty in large-scale forcings, Fridlind et al. (2012) results indicate that known physics can go far. That said, it should be noted that different LES codes produce quite different results in the limit of fully liquid-phase conditions, consistent with warm cloud intercomparison studies (e.g., Ackerman et al., 2009, factor of 3 spread in LWP). Given fixed $N_i$ in this case, it is not surprising that LES additionally predict differing ice production rates. Among models that predict LWP within a factor of two in the BASE intercomparison simulation, predicted IWP varies by less than a factor of two, a relatively close agreement owing at least in part to strongly constrained $N_i$.

Finally, ice formation mechanisms remain unclear, and quantitative ice crystal properties are a requirement unmet by observational analyses thus far, as discussed further below.

## 3. ISDAC CASE STUDY

As discussed by Avramov et al. (2011), flights 16 and 31 respectively on Apr. 8 and 26, 2008 during the ISDAC campaign both sampled widespread, single-layer, mixed-phase stratocumulus decks over pack ice with cloud bases colder than $-8°C$ (Fig. 1). In both cases, soundings indicate a relatively well-mixed cloud layer of roughly 0.5 km depth with cloud-top temperatures around $-15°C$ overlying a stable, moister surface layer of similar depth, and relatively uniform horizontal wind speeds of $7-9$ m s$^{-1}$ (Avramov et al., 2011; Ovchinnikov et al., 2014). The Apr. 8 case was selected by Avramov et al. (2011) owing to the availability of ground-based remote-sensing data in the same cloud deck over the US Department of Energy Atmospheric Radiation Measurement Program's North Slope of Alaska site, whereas the Apr. 26 case was selected by Ovchinnikov et al. (2014) for a model intercomparison study. Owing to the close similarity of the cases and the greater availability of observations for the Apr. 8 case, we will discuss both here, roughly interchangeably, and use examples from the earlier case to illustrate some points. For instance, the ground-based MMCR time series from the earlier case is shown in Fig. 3.

Microphysically, conditions during both flights were characterized by a wide range of dendritic crystals and their aggregates (Fig. 6 and Avramov et al., 2011, their Fig. 4). Dendrites in both cases exhibited a wide range of arm properties, ranging from needle-like to plate-like to highly branched. In both cases, single crystals transitioned to aggregates with increasing maximum dimension, over an estimated size range of 1–4 mm in the Apr. 8 case (Avramov et al., 2011). In other words, crystals smaller than 1 mm were predominantly unaggregated and those larger than 4 mm predominantly aggregated. The aircraft did not extensively sample elevations below roughly 0.5 km (e.g., Avramov et al., 2011, their Fig. 15), where sublimation was also an active process (e.g., Ovchinnikov et al., 2014, their Fig. 18).



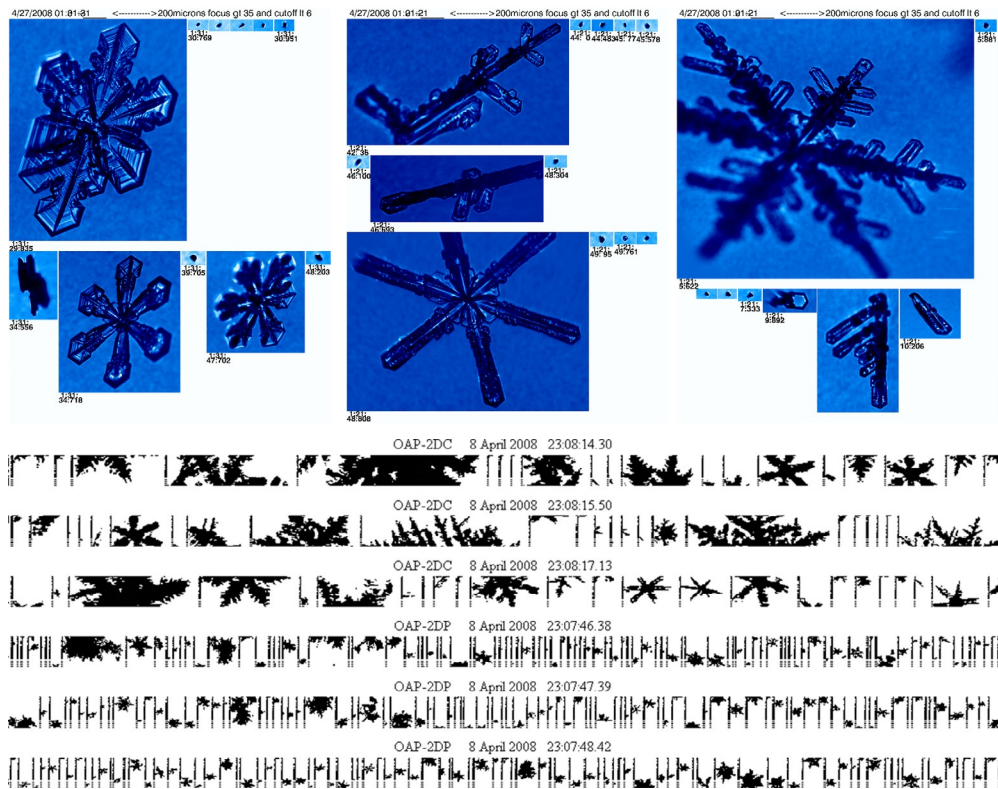**Fig. 6** CPI data from the ISDAC intercomparison case study observation period (flight 31) show primarily unrimed dendrites with a wide range of arm thickness and branch patterns. Two-Dimensional Cloud and Precipitation (2DC and 2DP) Optical Array Probe (OAP) data from similar conditions during flight 16 show similar dendrites and their aggregates. The vertical dimension of 2DC and 2DP images is ∼1 mm and 6 mm, respectively.

## 3.1 Intercomparison Specification

A bimodal PSD of ammonium bisulfate aerosol was specified for models that treat droplet activation, and a fixed droplet number concentration of 200 cm$^{-3}$ was specified for the rest. As in the Morrison et al. (2011) intercomparison, Ovchinnikov et al. (2014) sought to constrain ice nucleation for the purposes of intercomparison by controlling $N_i$ within cloud to be zero (liquid–phase only), 1 L$^{-1}$, based loosely on observations, and 4 L$^{-1}$. Going further than any previous specification to our knowledge, ice crystal properties were also specified in detail, including the relationships among mass, crystal maximum dimension, capacitance, and fall speed. Aggregates were neglected for simplicity. As recommended by the Morrison et al. (2011) study, the onset of ice formation was delayed until after a 2–h liquid–phase spin–up.

Unlike the other case studies, large–scale forcings were not specified based on reproducing evolution of boundary layer thermodynamics for a specified baseline. Rather, large–scale subsidence was selected in a manner that led to minimal cloud–top height evolution, whereas moisture and temperature, as well as zonal and meridional winds above the inversion, were nudged with 1 h and 2 h time scales, respectively. For thermodynamic quantities, 1–h nudging was not sufficient to avoid substantial evolution of the profile away from the observed decoupled state of the boundary layer toward a well–mixed state. LWP and dynamical properties of the cloud–topped and surface layers evolved in a manner similar to that also shown in the Avramov et al. (2011) ISDAC simulations, as discussed further below.

## 3.2 Intercomparison Results

Considering first liquid–phase only conditions, all participating LES models predicted a rapid increase of LWP from roughly 10 to 50 g m$^{-2}$ over 8 h. The models that predicted a most rapid LWP increase were those that most rapidly deepened the cloud–topped layer downwards into the surface layer, reaching the surface and leading to a relatively well–mixed state within roughly 4 h. Those models with the slowest increase of LWP reached maximum LWP at roughly 7 h. Since these results are without ice, they indicate a relatively wide range of LES dynamical behavior with relatively simple microphysics (no drizzle, relatively high droplet number concentration).

In simulations with ice formation beginning at 2 h, $N_i = 1$ L$^{-1}$ had a relatively weak desiccating effect for most models and 4 L$^{-1}$ a greater effect. Despite the fact that they produce grossly differing rates of boundary layer coupling, the two models with independent size–resolved, bin microphysics schemes were shown to produce the greatest IWP and ice diffusional growth rates. In the case of $N_i = 4$ L$^{-1}$ those two models also produced closely similar evolutions of IWP.

Through detailed comparison of bulk and bin microphysics and additional sensitivity tests, Ovchinnikov et al. (2014) demonstrate that the bin microphysics schemes prognose

PSD features that lead to systematically more ice than bulk schemes. By fitting gamma size distributions to the bin results, it is further demonstrated that ice size distributions are narrower than the exponential shape typically assumed in bulk schemes. When these factors were accounted for, for instance by specifying in the bulk schemes a gamma size distribution shape parameter calculated from the size distributions obtained using bin microphysics, then the bulk and bin schemes were brought into quite close agreement. Thus once ice individual-crystal properties are fully specified, it is found that ice size distribution shape is also an important determinant of mixed-phase cloud evolution. In this case over 6 h of ice formation, using an exponential size distribution led to roughly twice as much LWP as predicted with a bin scheme's fitted gamma shape parameter of roughly 3.

## 3.3 Related Studies

In a follow-on study focused on boundary layer dynamics for the Apr. 26 case, Savre et al. (2014) suggest a dominant role for near-surface large-scale advection of cold air in maintaining a decoupled cloud-topped boundary layer, consistent with ISDAC observations and in contrast to LES of both the Apr. 8 case (Avramov et al., 2011, their Fig. 20) and the Apr. 26 case (Ovchinnikov et al., 2014, their Fig. 2), which did not include such large-scale forcings. They explore factors that favor maintenance of cloud-topped layer decoupling commonly observed in the Arctic, including the role of a humidity inversion (i.e., increase with height) at cloud top (e.g., Curry, 1986), which is unknown in warm stratocumulus (e.g., Ackerman et al., 2004).

Avramov et al. (2011), Solomon et al. (2015), and Savre and Ekman (2015b) all examine the IFN budget in the context of LES and mesoscale modeling studies, each with a slightly differing emphasis and approach. In contrast to the SHEBA case conditions, ice sublimation is an active process in all of the ISDAC case studies, but the studies reach varying conclusions regarding the role of IFN recycling.

Avramov et al. (2011) seek to reconcile in situ IFN measurements via CFDC with in-cloud $N_i$. If cloud-top entrainment were the only source of rapidly activated IFN, they find $N_{IFN}/N_i$ to be at least 50, reflecting the cloud-top entrainment limitation discussed above, inconsistent with the factor of 10 observed (roughly 10 L$^{-1}$ IFN and 1 L$^{-1}$ $N_i$). If $N_{IFN}$ are similar in the surface layer below and that air is entrained substantially from the bottom of the cloud-topped mixed layer, they report that $N_{IFN}$ measured could potentially explain $N_i$ observed. However, as already noted, such rapid entrainment of below-cloud air in their simulations is not consistent with observations. They also report that sublimation of ice is a potential source of IFN, but only to a shallow surface layer that likely did not play a role during the observation period.

Solomon et al. (2015) consider a longer integration period of 40 h in mesoscale model simulations of the Apr. 8 conditions. They find that a subcloud layer that is well-stocked with IFN can serve as a persistent reservoir of IFN when the cloud is continually

entraining from such a source beneath the mixed-layer base. In a simulation without recycling, the cloud layer deepening entirely depletes the surface layer as it mixes out. In a simulation with recycling, the surface layer is initially enriched in IFN, as in Avramov et al. (2011), and the layer serves as an efficient source if it is efficiently mixed out.

Savre and Ekman (2015b) reach an entirely different conclusion, namely that IFN recycling scarcely matters to predicted IFN in several ISDAC case studies. Rather than initializing $N_{IFN}$ using CFDC measurements and assuming that such IFN are all rapidly nucleated, as did Avramov et al. (2011) and Solomon et al. (2015), Savre and Ekman (2015b) assign a distribution of contact angles to measured dust and soot aerosol concentrations. They conclude that cloud-top entrainment of IFN is responsible for only roughly 25%–40% of ice formed during 6 h simulations. In their simulations with a contact angle distribution, cloud top cooling that is accompanied by rising cloud top in all three of their case studies leads to nucleation of an increasing number of dust and soot IFN present initially within the cloud layer. In addition, they stress that the distribution of contact angles assigned to IFN is required to explain persistent ice formation because the more weakly active IFN help to sustain steady ice nucleation rates as discussed further below.

## 3.4  ISDAC Lessons

Relative to the other campaign cases, ISDAC studies were complicated by the representation of boundary layer decoupling and cooling of cloud top in simulations. Most simulations studied included cooling of cloud top but arguably none well demonstrated that they reproduced observed cloud-layer decoupling behavior compared with observations.

Given a cloud-topped boundary layer hosting ice production, Ovchinnikov et al. (2014) demonstrated that independent bin microphysics schemes agreed with one another when ice properties were completely specified, and demonstrated that bulk simulations could be brought into agreement with the bin simulations when the assumed gamma shape parameter was specified based on results from the bin simulations. Avramov et al. (2011) demonstrated that ice properties, such as those specified by Ovchinnikov et al. (2014), could not be readily derived from observations owing to a large diversity of dendrite shapes present. In short, no quantitative analyses were available to constrain the specified ice properties.

Regardless of dendrite habit selected by bracketing the habit range observed, Avramov et al. (2011) also demonstrated that a size-resolved microphysics scheme can accurately predict the transition from single crystals to aggregates with increasing size. Simulations agreed best with observed in situ measurements of ice PSD and remote-sensing measurements of X-band $Z$, and $V_f$ and W-band $Z$, when ice crystals and their aggregates were assumed to be composed of low-density elements (with thin arms). Aggregates were important to proper prediction of $Z$, but scarcely reduced $N_i$ and only modestly reduced IWP and slightly increased LWP.

Modeling studies arrived at diverse and conflicting conclusions regarding ice formation. Avramov et al. (2011) attempted a study of $N_i$–$N_{IFN}$ closure using CFDC measurements, and came to the tentative conclusion that observed IFN could explain observed $N_i$ if substantial entrainment of surface layer IFN were invoked, but observations were not available to establish what occurred and simulations likely overestimated entrainment of surface layer air. Savre and Ekman (2015b) also came to the tentative conclusion that observed aerosol properties could explain observed ice properties, but results were sensitive to assumed aerosol ice nucleating properties and were not constrained by CFDC measurements. Solomon et al. (2015) concluded that recycling was a chief factor sustaining $N_i$ whereas Avramov et al. (2011) and Savre and Ekman (2015b) found otherwise for entirely differing reasons, as discussed further below.

Finally, it is notable that no studies considered a role for ice multiplication under ISDAC conditions, or, to our knowledge, for blowing snow or any source excepting primary ice nucleation via activation of IFN.

## 4. M-PACE CASE STUDY

The M–PACE case study observation period took place during an extended cold–air outbreak over the open Beaufort Sea (Fig. 1). During Oct. 8–12, cloud–top temperatures at Barrow fell from roughly −10°C to −17°C (cf. Fridlind et al., 2007, their Fig. 2). In contrast to the negligible surface turbulent heat fluxes over pack ice in the SHEBA and ISDAC cases, clouds rapidly approaching Barrow from the Beaufort Sea with horizontal wind speeds of roughly 13 m s$^{-1}$ were fed by sensible and latent heat fluxes both in excess of 100 W m$^{-2}$, yielding LWP in excess of 100 g m$^{-2}$ and correspondingly substantial IWP on the order of 10 g m$^{-2}$ (Klein et al., 2009). Roll convection common to such cold-air outbreaks was evident in high-resolution imagery (cf. Klein et al., 2009, their Fig. 1), characterized by increasing roll aspect ratio with distance from the ice edge (e.g., Gryschka and Raasch, 2005, and references therein). Undulations in cloud top height seen by radar at Barrow may have been associated with meandering of roll structures (Fig. 3). The high LWP in combination with low droplet number concentration of 30–40 cm$^{-3}$ led to active drizzle and riming processes evident in CPI data (Fig. 7).

### 4.1 Case Study Specification

As described by Klein et al. (2009), idealized initial thermodynamic and wind profiles were based on soundings at Barrow, with a fixed-temperature ocean surface. Idealized large-scale forcings were derived from reanalysis results 200 km upwind of Barrow. Models were to use their own interactive radiative fluxes with solar zenith angle varying realistically as a function of time, as in the SHEBA intercomparison and in contrast to the more constrained parameterized treatment used in the ISDAC case. Sensible and latent heat fluxes were fixed as in both SHEBA and ISDAC cases to increase constraint on models diverging for reasons other than cloud dynamics or microphysics, in this case
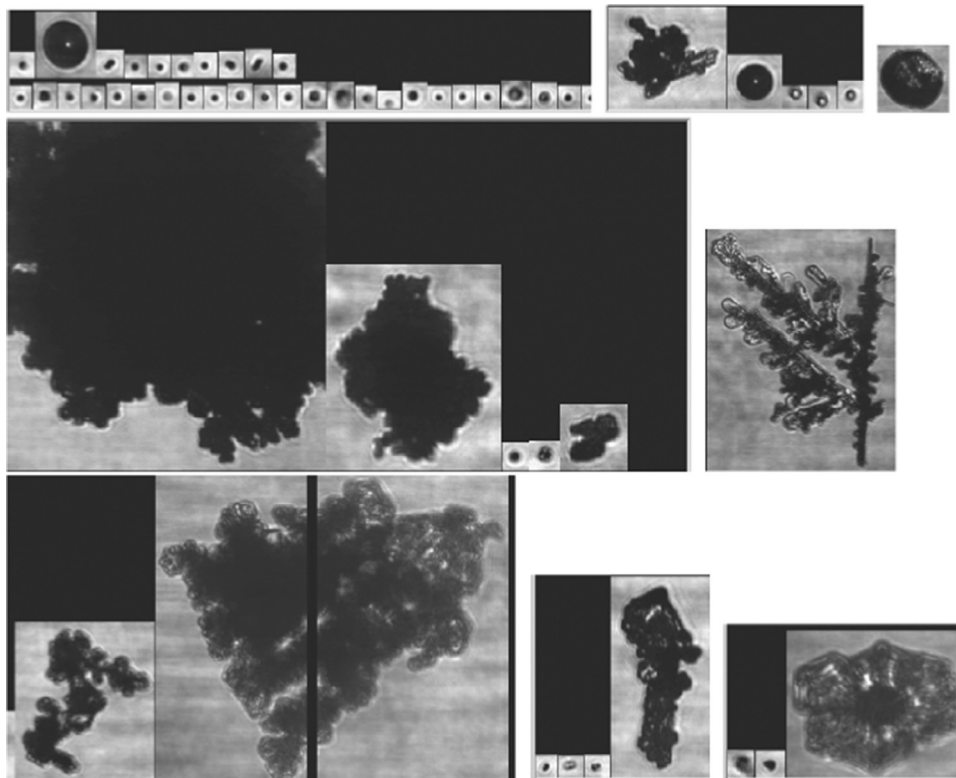
**Fig. 7** CPI data from the Oct. 9–10 flights during M-PACE show a wide range of properties, from lightly to heavily rimed and from plate-like to spatially branched. Drizzle drops are relatively common near cloud base (top), but to our knowledge only one single image captured a pristine frozen drizzle drop (upper right).

to 110 and 140 W m$^{-2}$, respectively, based on reanalysis. A bimodal aerosol size distribution with accumulation and coarse modes was specified based on derivation from Barrow CCN data and a handheld particle counter mounted on an Aerosonde UAV (Morrison et al., 2008). An IFN concentration of 0.16 L$^{-1}$ was reported (but its use not specified), based on CFDC measurements under varying above- and within–cloud conditions, which was noted to be close to the CFDC detection limit of roughly 0.1 L$^{-1}$.

## 4.2 Intercomparison Results

The intercomparison included a range of 2D eddy-resolving models and 3D LES and other cloud-resolving models (CRMs), as well as single-column models (SCMs). Results were not identified by model, and only classified by the microphysics scheme complexity.

From our knowledge of our submission based on code described in Fridlind et al. (2007), we can distinguish between the 2D and 3D bin microphysics simulations in the following discussion, but are otherwise limited in our ability to distinguish 2D from 3D bulk microphysics simulations.

Among the CRM results, in contrast to the SCM results, essentially all simulations maintained a mean mixed-phase boundary layer cloud depth of 1.5 km. However, that is where similarities ended. Median predicted LWPs ranged from roughly 0 to 175 g m$^{-2}$ compared with an observational range of roughly 110–210 g m$^{-2}$. Only three of nine CRMs maintained LWP within roughly a factor of 2 of that observed, and most grossly underpredicted LWP. With an exception or two—one of which is a 2D model in the case of bin microphysics—simulated IWP was roughly anticorrelated with LWP in CRMs. Thus underprediction of LWP could be generally tied to overprediction of IWP, which can be understood as precipitation removal of LWP owing to overproduction of ice. Klein et al. (2009) emphasize that complexity of microphysics did not necessarily lead to improved performance, at least partly related to the fact that CRMs reported an astonishing five order of magnitude range of predicted $N_i$. The extreme diversity of results when specifying $N_{IFN}$ in this study led directly to the strong constraints applied essentially directly to $N_i$ in the SHEBA and ISDAC intercomparison studies.

We note that our LES submission to the intercomparison was based on simulations that included production of ice associated with evaporation of droplets, which we identified out of many proposals in the literature as one possible means by which $N_i$ might be maintained within the range of observations (Fridlind et al., 2007). A possible surface source of IFN or an unknown ice multiplication mechanism were identified as other possibilities. Without that ad hoc ice production mechanism, our simulations would have reported essentially negligible IWP, as discussed further below, and LWP similar to the no-ice sensitivity test discussed by Klein et al. (2009). It is notable that CRM simulations without the ice phase already differed by more than a factor of three; 2D versus 3D could play some role in that. This diversity can be considered quite surprising since the case study is relatively simple from the standpoint that turbulence is robust and the boundary layer is relatively well-mixed throughout.

## 4.3 Related Studies

Here we will focus on two related studies that included detailed microphysics with prognostic IFN in 3D simulations. The significance of a prognostic instead of diagnostic treatment of IFN is that the former allows consumption of IFN upon nucleation of an ice crystal. In contrast, the latter does not deplete the abundance of IFN available for further nucleation and thus will tend to result in greater ice crystal formation rates by virtue of ignoring the basic fact that once an IFN is within an ice crystal it is no longer available for further primary nucleation. Aggregation of ice crystals that form on IFN will reduce the

number of IFN returned to the atmosphere upon complete sublimation of the aggregate, and sedimentation of ice formed on IFN will also serve as a sink of IFN.

Fridlind et al. (2007) focused primarily on the gross inability of observed IFN to explain observed $N_i$. In that study, when specifying thermodynamic soundings and winds based on a Barrow sounding and sea surface temperature offshore with an ocean surface and predicted latent and sensible heat fluxes, it was first found that the liquid phase cloud properties could be roughly reproduced without difficulty. Drizzle was not well constrained by observations but was predicted and seen in observations as discussed above. However, IFN that were based on CFDC measurements and were, by extension, considered to be rapidly nucleated, were quickly consumed. As noted by Fridlind et al. (2007), this IFN consumption process was well described by Harrington and Olsson (2001) based on their earlier simulations of similar conditions. Fridlind et al. (2007) furthermore reported that assuming CFDC-observed IFN to be fully restored and available for reactivation upon sublimation made little difference. Given that $N_i$ was estimated at $10\ L^{-1}$ and was clearly visible precipitating to the surface in radar measurements, it is not surprising that IFN could not build up far beyond the $0.2\ L^{-1}$ value observed and could not possibly account for $10\ L^{-1}$ ice, even when considering an estimated factor of 5 uncertainty in observed $N_i$.

In response to this, Fridlind et al. (2007) sought possible mechanisms to explain the M-PACE ice observations in decades of literature, which also documented evidence of such discrepancies in both stratiform and cumuliform clouds. Chief among these were several ice multiplication mechanisms, which Fridlind et al. (2007) found insufficiently effective in simulations, conceivably in part owing to a lack of properly specified ice properties, as discussed further below. Other possibilities identified were an ocean surface source of IFN or potential physicochemical changes in droplet residuals, for instance associated with collision-coalescence of droplets containing biogels (Leck and Bigg, 2005) with those containing sulfate, which could lead to exposure of ice-nucleating solids. Now as then, all of these possible processes remain unproven, although the ocean is increasingly viewed as a relatively weak source of IFN (e.g., Demott et al., 2016). An ice multiplication mechanism involving the coexistence of fragile and dense ice has been further investigated (Yano and Phillips, 2011), and the potential of large freezing droplets to produce more ice splinters than previously established may also emerge from new laboratory measurements (e.g., Lawson et al., 2015).

Using an independent LES code with an independent size-resolved microphysics scheme, Fan et al. (2009) largely confirmed the basic findings of Fridlind et al. (2007) insofar as the gross inability of observed IFN to account for observed ice. However, Fan et al. (2009) make the additional point that IFN recycling can become important when IFN are as abundant as required to sustain observed $N_i$, for instance via a within-droplet physicochemical process. Fan et al. (2009) also illustrate that even when $N_i$ in simulations is substantially increased by some additional mechanism,

forward-simulated $Z$ remains low compared with MMCR. This is important to consider since observations of ice crystal number size distribution remain extremely uncertain owing to poorly established artifacts from crystals shattering on probes as well as difficulties establishing fundamental probe calibration (e.g., Baumgardner et al., 2011; Korolev et al., 2011). In other words, comparison of forward simulations of $Z$ from measured PSDs and $Z$ and $V_D$ from model results are helpful to support conclusions regarding consistency between simulated and observed ice loading when in situ measurement uncertainties are great (e.g., Fan et al., 2009; Avramov et al., 2011; Fridlind et al., 2012).

## 4.4 M-PACE Lessons

M-PACE demonstrated the potential for severe lack of model skill in simulating, and perhaps also observing, mixed-phase boundary layer clouds. On the observation side, at least M-PACE conditions closely conformed with those encountered on earlier airborne surveys of moderately supercooled stratiform clouds with large droplets and copious ice (Rangno and Hobbs, 2001), as discussed further below. On the modeling side, on the other hand, an intercomparison study produced five orders of magnitude difference in $N_i$ and the most detailed studies with prognostic IFN reported essentially no ability to explain $N_i$ far exceeding $N_{IFN}$ with known microphysical mechanisms. Perhaps underemphasized in this earliest of three case studies was the role of ice properties. Avramov and Harrington (2010) demonstrated that their simulations were strongly sensitive to assumed ice habit, but did not attempt to constrain their habit assumptions with in situ observations. As evidenced by the variety of shapes shown in Fig. 7, doing so would not have been an easy task.

## 5. DISCUSSION

We take the non-controversial view that parameterization efforts are hampered by lack of understanding of fundamental microphysical processes. In the following discussion, we therefore discuss the greatest microphysics knowledge gaps across these several case studies and identify outstanding questions.

## 5.1 Persistence and Strength of Ice Production

A central feature of all three observed case studies summarized here is persistent ice formation, as evidenced clearly by cloud radar (Fig. 3). Essentially none of the simulations with detailed microphysics and prognostic IFN fail to reproduce persistent ice formation, with the possible exception of some reported by Klein et al. (2009). However, the simulations tend to not produce sufficient ice, most extremely so in the M-PACE case.

Although observed ice loadings often appear to be substantially greater than can be explained by collocated IFN measurements and known physics, the evidence that it is sufficient to rapidly glaciate available LWP is not strong. Ice consistent with that observed appears to be playing a relevant role in the mixed-layer water budget, but it is not the dominant player that is seen when $N_i$ is made extraordinarily greater than observed in SHEBA intercomparison sensitivity test simulations discussed above, for instance.

Prior to all the case study work described above, this central feature of continuous ice formation was already well identified in the Morrison et al. (2005) study of SHEBA conditions where a role for contact freezing was proposed to explain it. The role of IFN consumption in limiting persistent ice production was also previously identified by Harrington and Olsson (2001).

In short, what the modeling and analysis of these case studies suggest is that CFDC measurements of IFN and known physics going into models seem inadequate to explain observed ice. Results are most inconsistent in the M-PACE case, when drizzle and riming are also active and a poorly known or even unknown multiplication process appears likely to play a powerful role. That said, ice consistent with observations then plays a greater role in the water budget, but still remains far from glaciating such clouds because the conditions consistent with multiplication in the observed M-PACE case also happen to be those where there is no shortage of water vapor with such a strong surface vapor flux. The two conditions are related since a latent heat flux in the M-PACE case leads to a substantial LWP, contributing to active drizzle and riming, which appear implicated in multiplication (e.g., Rangno and Hobbs, 2001). It also seems possible that such a multiplication process could be self-limiting in the sense that if explosive ice formation were to substantially reduce LWP, then the ice formation itself would also be slowed.

## 5.2  Primary Ice Formation

It is natural to begin discussion of ice formation with the idea that there are cases where ice multiplication is not active. The limiting case of very low LWP and relatively high $N_d$ as in the SHEBA case could be representative of such conditions. Under such conditions, de Boer et al. (2011) have convincingly argued that ice formation appears to accompany the presence of liquid water, as in condensation, immersion, or contact freezing. They base that on analyses of collocated lidar and radar measurements that show reflectivity associated with ice formation and growth increasing only after supercooled cloud water is seen by lidar. Thus available IFN under moderate supercooling appear to require a liquid phase or at least water saturation to be activated, which is consistent with the laboratory finding that IFN are orders of magnitude more active above water saturation than below in CFDC measurements (e.g., Sullivan et al., 2010, their Fig. 1).

Using prognostic IFN with a singular treatment (in which activation occurs instantaneously upon attaining specified conditions (cf. Phillips et al., 2008)), Fridlind et al.

(2012) found in simulations that contact IFN behaved fundamentally differently from IFN acting in other modes. Namely, a boundary layer full of contact IFN that could be activated under cloud-top conditions would be only slowly depleted from the boundary layer because contact between IFN and droplets served as a rate-limiting step that proceeds so slowly an initial boundary layer reservoir of IFN present before cloud formation could produce ice continuously and steadily for tens of hours. This contrasted with IFN assumed to act in other modes where conditions within the boundary layer would guarantee activation and depletion of the whole boundary layer IFN reservoir within roughly 1 h and sedimentation of all ice crystals on a similar time scale.

Fridlind et al. (2012) therefore refer to non-contact IFN as rapidly nucleated, consistent with measurements made with a CFDC instrument, which has an effective residence time of roughly 4 s (Paul DeMott, personal communication). Fig. 8 illustrates the differing behaviors of a reservoir of rapidly activated versus slowly activated IFN, using contact
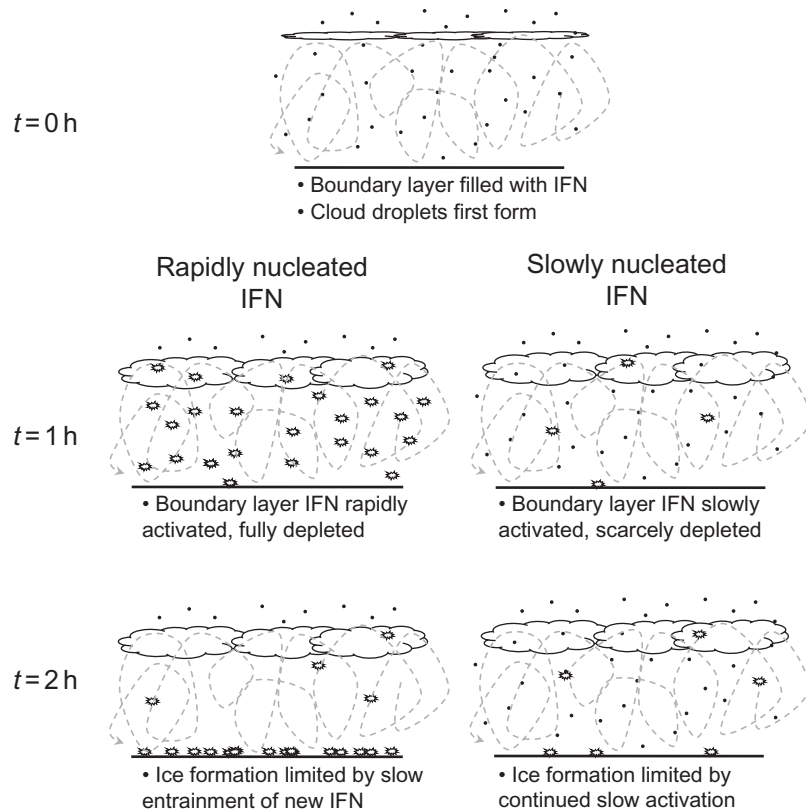


**Fig. 8** Illustration of IFN progression in SHEBA case study simulations with rapidly nucleated IFN (left) and slowly nucleated IFN (right), as in the "Prognostic IN" and "Contact IN only" simulations reported by Fridlind et al. (2012).

IFN as example of slowly nucleated particles. It should be noted that if an initial boundary layer reservoir of IFN are entirely and quickly depleted, water vapor will be substantially depleted if the initial concentration is high enough. For instance, in order to avoid rapid LWP depletion in Fridlind et al. (2012) with 50 $L^{-1}$ IFN in the SHEBA case, simulations had to be initialized with steady-state depleted levels within the boundary layer, allowing the entrainment source of IFN to slowly balance its surface loss rate.

Savre and Ekman (2015b) report simulations of ISDAC case studies, discussed above, where slow IFN nucleation proceeds via the immersion mode rather than the contact mode. Using a time-dependent (nonsingular) treatment of IFN based on classical nucleation theory (Savre and Ekman, 2015a), they assign a distribution of contact angles to the dust and soot particles estimated from in situ single-particle observations, further subject to population fractions of two-thirds and one-third able to act as IFN, respectively. They arrive at a substantial reservoir of potential IFN in the boundary layer, at least two orders of magnitude greater than observed by CFDC with a 4 s residence time. By following the contact angle distribution prognostically, they find that that substantial reservoir sustains $N_i$ similar to that observed in all three cases, aided by cooling of cloud top, whereas a singular treatment of the IFN fails to do so.

The idea that many IFN may be relatively weakly active or may be active only in the contact mode—in either case slowing their depletion and providing a steady source of ice—was also suggested by Westbrook and Illingworth (2013). In a well observed decoupled mixed-phase cloud layer with stable cloud-top temperature, they argue that cloud top and cloud base entrainment are both negligible and that some type of slow activation process must be required to sustain the ice observed. Based on budgets of $N_i$ flux estimated from observations, they also report that sustaining ice for tens of hours would require more IFN than ever reported by CFDC measurements in the immersion mode. In other words, not only was slow activation required to explain their data, but an IFN source beyond that commonly understood to be present in the atmosphere was also required.

One reason it may be difficult to distinguish how nucleation is proceeding is that very different spatial distributions of nucleation could lead to similar occurrence of a relatively uniform distribution of $N_i$ when averaged horizontally. For instance, in SHEBA case study simulations where nucleation is concentrated at cloud top or is distributed throughout the liquid cloud layer (Fig. 9), the horizontal mean $N_i$ fields are similarly uniform vertically owing to turbulent mixing, as demonstrated in Fridlind et al. (2012, their Fig. 10). Yang et al. (2013) proposed that examining the underlying relationship of $N_i$ and ice mass mixing ratio ($q_i$) could give insight into where the nucleation is occurring, as well as the underlying rate. Fig. 10 shows such the differing patterns of $N_i$ versus $q_i$ below cloud base for a SHEBA case study simulation, which are similar to those within-cloud but likelier easier to observe. They differ somewhat from those reported by Yang et al. (2014) for an ISDAC case study with cloud-top seeding.
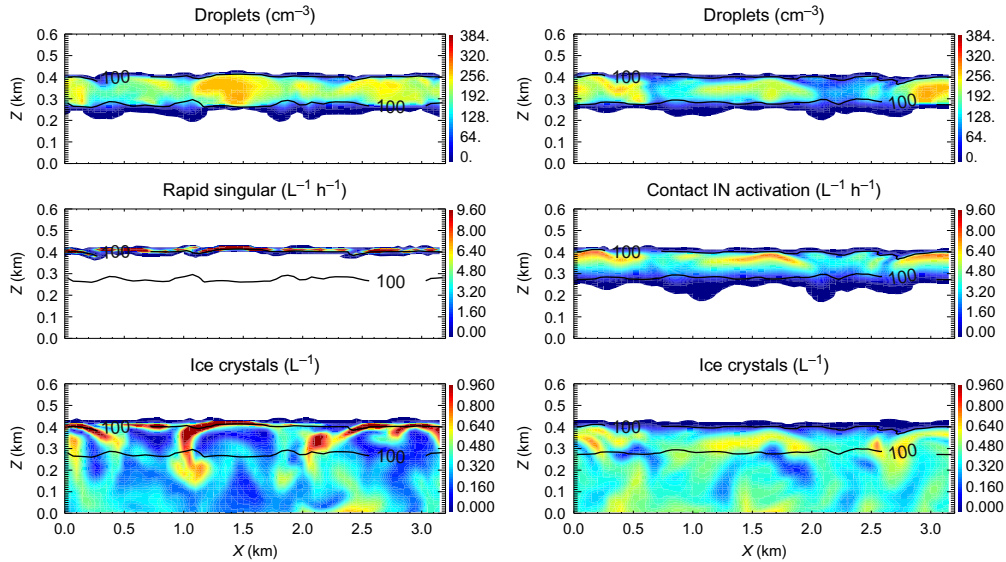
**Fig. 9** Cross-section of $N_d$, IFN activation rate, and $N_i$ in simulations with rapidly nucleated IFN (left) and slowly nucleated IFN in the contact mode (right), as in the "Prognostic IN" and "Contact IN only" simulations reported by Fridlind et al. (2012).
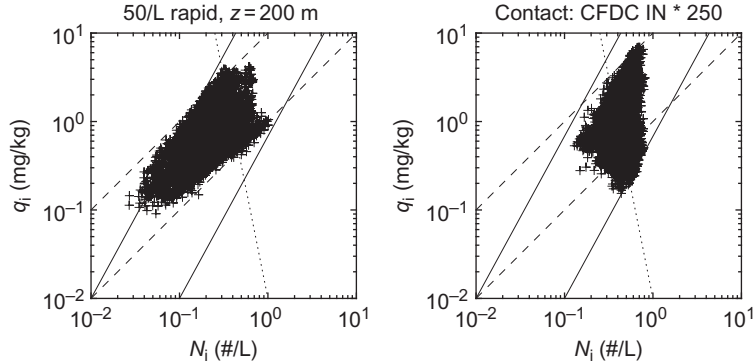


**Fig. 10** Ice mass mixing ratio ($q_i$) versus number concentration ($N_i$) at an elevation of 0.2 km in simulations with rapidly nucleated IFN (left) and slowly nucleated IFN in the contact mode (right) shown in Fig. 9, as in the "Prognostic IN" and "Contact IN only" simulations reported by Fridlind et al. (2012). Lines following slopes of 1, 2.5, and −5 following Yang et al. (2013, 2014) drawn for comparison.

Recently it has been reported that CFDC measurements may underestimate IFN by a factor 2–10 owing to their exclusion of aerosol with diameter exceeding roughly 1.5 μm (Mason et al., 2016), and the bias increases at warmer temperatures. This under-counting could actually exacerbate rather than diminish a curious feature of Arctic IFN from CFDC measurements, namely a pronounced weak dependence on temperature

(e.g., Prenni et al., 2007). Unlike Savre and Ekman (2015b), in part owing to a focus on CFDC measurements as an observational constraint, Fridlind et al. (2012) and Avramov et al. (2011) neglected or underestimated the contribution of increasing IFN available owing to progressive cooling of cloud top. In the ISDAC cases, aircraft observations clearly indicate that cooling of cloud top is relatively rapid on Lagrangian flight legs. We are unaware of analysis of the downwind evolution of cloud-top temperatures for the M-PACE or SHEBA cases. It is also not clear the degree to which assumptions made by Savre and Ekman (2015b) in ISDAC cases are consistent with ISDAC CFDC measurements when applying the CFDC residence time and aerosol diameter sampling limitations.

While it is beyond the scope of this chapter to review the somewhat recent explosion of studies of ice nucleation since the first case study discussed here, we can at least identify some aspects of recent debate. For instance, recent conclusions regarding the importance of time dependence in measuring, reporting, and modeling primary ice nucleation have been notably diverse. For instance, Wright et al. (2013) concluded that neglecting time dependence in measurements leads to minimal error in reported IFN properties and that models will be correspondingly insensitive to inclusion of time dependence. On other hand, Herbert et al. (2014) concluded that time dependence is more important for some nucleating materials than others and recommend an approach to (i) reconcile measurements with differing cooling rate or residence time procedures and (ii) include it in models.

Some have also emphasized that IFN diversity within a given well-defined class (e.g., Arizona test dust) may be of negligible importance compared with adequately constraining sample aerosol surface area (Alpert and Knopf, 2016) whereas others argue that diversity is required to explain the freezing behavior of some materials but not others (Herbert et al., 2014). These factors become entwined when considering that isothermal experiments with diverse particles lead to extended IFN lifetimes owing to the slower freezing behavior of less efficient particles (e.g., Herbert et al., 2014, their Fig. 7). Savre and Ekman (2015b) emphasize this latter factor in explaining persistent ice formation in their ISDAC simulations that assume diverse nucleating efficiencies of dust and soot particles based on laboratory measurements. Since tracking such diversity introduces a non-negligible cost to simulations, it would present a major benefit if such schemes could be suitably reconciled with CFDC measurements under field conditions and collocated field measurements with instruments using substantially longer residence times than the CFDC.

In a climate-model study reporting implementation of a relatively complex time-dependent IFN nucleation scheme, it was concluded that sensitivity to time dependence is weak compared with other IFN properties whose values remain profoundly uncertain (Wang and Liu, 2014). For instance, recent intercomparisons of IFN measurement techniques for a material reported very weakly time dependent remains three orders of magnitude apart in activity or 8°K, and differences are most pronounced at the warmer temperatures similar to those in the case studies discussed here (Hiranuma et al., 2015).

Finally, it is relevant that a consensus seems to be building across the community that immersion freezing is the dominant ice formation process in supercooled clouds (Vali and Snider, 2015), but it could be premature to rule out a role for contact freezing specifically in very long-lived supercooled clouds owing to uncertainties in contact rates (e.g., Ladino Moreno et al., 2013).

## 5.3  Secondary Ice Formation

By definition secondary ice formation must be initiated by some primary ice nucleation, and is thought to increase $N_i$ by an order of magnitude or more (e.g., Pruppacher and Klett, 1997, and references therein).

The only ice multiplication mechanism widely included in current microphysics schemes is Hallett–Mossop rime-splintering. Based on laboratory experiments, that process requires riming by droplets with diameter greater than 24 μm on an ice hydro-meteor with a surface temperature of −3°C to −8°C (Pruppacher and Klett, 1997). Across these case studies, it is notable that ice formation is greatest by far in the M-PACE case, with large droplets and an active riming process, despite cloud base temperature colder than the Hallett–Mossop temperature range. This common scenario has led many to conclude that an unknown or poorly constrained ice multiplication mechanism is likely active under such conditions (e.g., Morrison et al., 2008), as originally surmised by Rangno and Hobbs (2001) in explaining their survey of slightly to moderately supercooled clouds of varying droplet number concentration and varying active processes.

In particular, Rangno and Hobbs (2001) identify riming and splintering as processes that accompany the production of a droplet effective radius exceeding 12 or 20 μm within a stratiform cloud that is supercooled by 10 or 20°C, respectively, and find contrasting conditions of weak ice formation otherwise. It could be the case that ice multiplication under such conditions is either dependent upon the production of splinters by the freezing process of large droplets, as suggested by Lawson et al. (2015), or is dependent on the production of splinters by ice-ice collisions, as suggested by Yano and Phillips (2011). In the latter case, the process could be substantially dependent upon ice properties. For instance, a detailed observational study found that at least 20% of dendrites had undergone natural fragmentation as evidenced by partial regrowth under conditions similar to the ISDAC case study (Schwarzenboeck et al., 2009). It is notable that relatively warm-temperature ice multiplication mechanisms are now being invoked to explain ice distributions emanating from updrafts within growing tropical cumulus (Lawson et al., 2015) and mature mesoscale convective systems (Ackerman et al., 2015; Fridlind et al., 2017), where conditions could be rather similar from the perspective of coexisting large droplets and ice with an active riming process.

It may be useful to separate the M–PACE conditions with likely ice multiplication from the SHEBA conditions of relatively negligible ice formation putting ISDAC perhaps closer to SHEBA than M–PACE. In the phase space of Fig. 2, fragmentation can be considered to increase with LWP, perhaps always accompanying aggregation or riming to some degree. Field studies of ice formation and multiplication require faithful measurements of PSDs, which brought to the fore concerns of severe contamination over several decades of $N_i$ measurements by ice shattering (Korolev et al., 2011). Perhaps suggesting that such concerns have been adequately addressed through instrument design and post–measurement analysis, arguments that observed IFN cannot explain $N_i$ at the level of repeated measurements and climatologies are again being put forth (e.g., Petters and Wright, 2015). Such conclusions are being driven by renewed emphasis on ice formation measurements (e.g., DeMott et al., 2011), which is leading to the advancement of measurement techniques for both $N_i$ and IFN, if not substantially greater confidence in either as of yet (e.g., Lawson, 2011; Baumgardner et al., 2012; Hiranuma et al., 2015).

## 5.4  Ice Crystal Properties

Variations among well–defined ice crystal habits can lead to substantial differences in water vapor budgets owing to differences in shape factor and sedimentation rate (e.g., Avramov and Harrington, 2010). In addition, it has been noted that ice crystal shapes observed in stratiform mixed-phase clouds are often highly irregular (Korolev et al., 2000), consistent with increasing polycrystalline forms and particle shape complexity, which has been observed to be associated with increasing ice supersaturation in the laboratory (e.g., Bailey and Hallett, 2004). In the context of supercooled mixed-phase clouds, increasing supersaturation is a natural consequence of decreasing temperature, where the relative humidity with respect to ice is increasingly supersaturated while relative humidity with respect to water remains essentially at the saturation value.

One way to understand the challenge for models is at the case study level. There, model setup can exploit CPI data, with a characteristic habit used for a given case study, and use crystal properties from the literature for that habit (e.g., Fridlind et al., 2012; Savre and Ekman, 2015b). However, as encountered by Avramov et al. (2011), habits such as dendrites may occur within the same cloud system in a wide range of forms that have quite dramatically different properties according to the literature. In short, at the case study level, there is currently an absence of quantitative information that can be used to assign relevant ice properties in a model that is designed to have those flexibly assigned or, much more challenging, predicted (e.g., Harrington et al., 2013). Furthermore, individual crystal mass was not systematically measured by any means during any of the field studies used here nor, to our knowledge, has it become a routine measurement in such studies since.

## 5.5  Climatology and Climate Sensitivity

We have discussed three case study conditions of shallow, single-layer mixed-phase cloud decks, all observed in the Arctic—one a cold-air outbreak over the Beaufort Sea in autumn and two over pack ice in spring. LES with detailed microphysics are able to reproduce basic aspects of all the case studies, including continuous ice formation within the context of a well-mixed liquid-cloud-topped layer. Microphysically, a chief open question is how the observed amount of ice is forming within such clouds. Assumed ice properties may also bear a significant influence on the water vapor budget and reflectivity properties. Active microphysical properties are related to ice properties insofar as riming and aggregation affect ice morphology.

Looking towards climate model parameterization, a leading question is whether these cases are representative of the shallow clouds that contain most of the radiatively important liquid at high latitudes and elsewhere that such clouds may be climatically relevant. Recent preliminary analyses of radar and lidar measurements at the North Slope of Alaska support the tentative conclusion that these case studies are representative of the most commonly occurring shallow mixed-phase clouds at that site. Namely, single-layer liquid-topped clouds represent about 72% of all shallow mixed-phase clouds observed during 2006–11, with the remaining occurrences being primarily characterized by more than one liquid-topped layer (23%) or multi-layer without liquid identifiable at the top of the uppermost layer (Katia Lamer, personal communication). Future work is aimed at establishing the frequency of active drizzle, riming, and aggregation processes. How often are these occurring and how important are they to the occurrence statistics for the radiatively important supercooled water?

If the North Slope of Alaska is a representative site for climatological significance, then it appears important to resolve immediately outstanding questions about ice formation. Is time-dependence important to include in models or not? Is it important to interpretation of observations? Does neglecting time dependence in a model serve to place the cloud state correctly or incorrectly into one of the two quasi-steady state conditions shown in Fig. 8, namely into a cloud-top entrainment limited state where recycling of IFN is more likely to be important, or into a state where a large initial reservoir of IFN is relatively slowly depleted? The role of cooling of cloud top in a deepening mixed-layer in a Lagrangian framework, as well as the understanding of whether and why immersion IFN may be so weakly temperature dependent under Arctic conditions, also deserves additional climatological evaluation.

## REFERENCES

Ackerman, A.S., Kirkpatrick, M.P., Stevens, D.E., Toon, O.B., 2004. The impact of humidity above stratiform clouds on indirect aerosol climate forcing. Nature 432 (7020), 1014–1017.

Ackerman, A.S., Stevens, B., Savic-Jovcic, V., Bretherton, C., Chlond, A., Hamburg, G., et al., 2009. Large-eddy simulations of a drizzling, stratocumulus-topped marine boundary layer. Mon. Weather Rev. 137, 1083–1110.

Ackerman, A.S., Fridlind, A.M., Grandin, A., Dezitter, F., Weber, M., Strapp, J.W., et al., 2015. High ice water content at low radar reflectivity near deep convection–Part 2: evaluation of microphysical pathways in updraft parcel simulations. Atmos. Chem. Phys. 15, 11729–11751.

Alpert, P.A., Knopf, D.A., 2016. Analysis of isothermal and cooling-rate-dependent immersion freezing by a unifying stochastic ice nucleation model. Atmos. Chem. Phys. 16 (4), 2083–2107. https://doi.org/10.5194/acp-16-2083-2016-supplement.

Avramov, A., Harrington, J.Y., 2010. Influence of parameterized ice habit on simulated mixed phase Arctic clouds. J. Geophys. Res. 115 (D3), D03205. https://doi.org/10.1029/2009JD012108.

Avramov, A., Ackerman, A.S., Fridlind, A.M., van Diedenhoven, B., Botta, G., Aydin, K., et al., 2011. Toward ice formation closure in Arctic mixed-phase boundary layer clouds during ISDAC. J. Geophys. Res. 116. https://doi.org/10.1029/2011JD015910.

Bailey, M., Hallett, J., 2004. Growth rates and habits of ice crystals between –20° and –70°C. J. Atmos. Sci. 61 (5), 514–544.

Baumgardner, D., Brenguier, J.-L., Bucholtz, A., Coe, H., DeMott, P., Garrett, T.J., et al., 2011. Airborne instruments to measure atmospheric aerosol particles, clouds and radiation: a cook's tour of mature and emerging technology. Atmos. Res. 102 (1-2), 10–29. https://doi.org/10.1016/j.atmosres.2011.06.021.

Baumgardner, D., Avallone, L., Bansemer, A., Borrmann, S., Brown, P., Bundke, U., et al., 2012. In situ, airborne instrumentation: addressing and solving measurement problems in ice clouds. Bull. Am. Meteorol. Soc. 93 (2), ES29–ES34. https://doi.org/10.1175/BAMS-D-11-00123.1.

Cober, S.G., Strapp, J.W., Isaac, G., 1996. An example of supercooled drizzle drops formed through a collision–coalescence process. J. Appl. Meteorol. 35, 2250–2260.

Comstock, K., Wood, R., Yuter, S., Bretherton, C., 2004. Reflectivity and rain rate in and below drizzling stratocumulus. Q. J. R. Meteorol. Soc. 130 (603), 2891–2918. https://doi.org/10.1256/qj.03.187.

Curry, J.A., 1986. Interactions among turbulence, radiation and microphysics in arctic stratus clouds. J. Atmos. Sci. 43 (1), 90–106. https://doi.org/10.1175/1520-0469(1986)043<0090:IATRAM>2.0.CO;2.

Curry, J.A., Hobbs, P.V., King, M.D., Randall, D., Minnis, P., Isaac, G.A., et al., 2000. FIRE Artic clouds experiment. Bull. Am. Meteorol. Soc. 81 (1), 5–29.

de Boer, G., Morrison, H., Shupe, M.D., Hildner, R., 2011. Evidence of liquid dependent ice nucleation in highlatitude stratiform clouds from surface remote sensors. Geophys. Res. Lett. 38 (1), L01803. https://doi.org/10.1029/2010GL046016.

DeMott, P.J., Prenni, A.J., Liu, X., Kreidenweis, S.M., Petters, M.D., Twohy, C.H., et al., 2010. Predicting global atmospheric ice nuclei distributions and their impacts on climate. Proc. Natl. Acad. Sci. U. S. A. 107 (25), 11217–11222. https://doi.org/10.1073/pnas.0910818107.

DeMott, P.J., Möhler, O., Stetzer, O., Vali, G., Levin, Z., Petters, M.D., et al., 2011. Resurgence in ice nuclei measurement research. Bull. Am. Meteorol. Soc. 92 (12), 1623–1635. https://doi.org/10.1175/2011BAMS3119.1.

Demott, P.J., Hill, T.C.J., McCluskey, C.S., Prather, K.A., Collins, D.B., Sullivan, R.C., et al., 2016. Sea spray aerosol as a unique source of ice nucleating particles. Proc. Natl. Acad. Sci. U. S. A. 113 (21), 5797–5803. https://doi.org/10.1073/pnas.1514034112.

Eidhammer, T., DeMott, P., Prenni, A., Petters, M., Twohy, C., Rogers, D., et al., 2010. Ice initiation by aerosol particles: measured and predicted ice nuclei concentrations versus measured ice crystal concentrations in an orographic wave cloud. J. Atmos. Sci. 67, 2417–2436.

Fan, J., Ovtchinnikov, M., Comstock, J.M., Mcfarlane, S.A., Khain, A., 2009. Ice formation in Arctic mixed-phase clouds: insights from a 3-D cloud-resolving model with size-resolved aerosol and cloud microphysics. J. Geophys. Res. 114, D04205. https://doi.org/10.1029/2008JD010782.

Fridlind, A.M., Ackerman, A.S., McFarquhar, G.M., Zhang, G., Poellot, M.R., DeMott, P.J., et al., 2007. Ice properties of single-layer stratocumulus during the mixed-phase arctic cloud experiment: 2. Model results. J. Geophys. Res. 112 (D24), D24202. https://doi.org/10.1029/2007JD008646.

Fridlind, A.M., van Diedenhoven, B., Ackerman, A.S., Avramov, A., Mrowiec, A., Morrison, H., et al., 2012. A FIRE-ACE/SHEBA case study of mixed-phase Arctic boundary layer clouds: entrainment rate limitations on rapid primary ice nucleation processes. J. Atmos. Sci. 69 (1), 365–389. https://doi.org/10.1175/JAS-D-11-052.1.

Fridlind, A.M., Li, X., Wu, D., van Lier-Walqui, M., Ackerman, A.S., Tao, W.-K., et al., 2017. Derivation of aerosol profiles for MC3E convection studies and use in simulations of the 20 May squall line case. Atmos. Chem. Phys. 17, 5947–5972. https://doi.org/10.5194/acp-17-5947-2017.

Gryschka, M., Raasch, S., 2005. Roll convection during a cold air outbreak: a large eddy simulation with stationary model domain. Geophys. Res. Lett. 32 (14), 1–5. https://doi.org/10.1029/2005GL022872.

Harrington, J., Olsson, P.Q., 2001. On the potential influence of ice nuclei on surfaceforced marine stratocumulus cloud dynamics. J. Geophys. Res. 106, 27473–27484.

Harrington, J.Y., Sulia, K., Morrison, H., 2013. A method for adaptive habit prediction in bulk microphysical models. Part I: theoretical development. J. Atmos. Sci. 70 (2), 349–364. https://doi.org/10.1175/JAS-D-12-040.1.

Herbert, R.J., Murray, B.J., Whale, T.F., Dobbie, S.J., Atkinson, J.D., 2014. Representing time-dependent freezing behaviour in immersion mode ice nucleation. Atmos. Chem. Phys. 14 (16), 8501–8520. https://doi.org/10.5194/acp-14-8501-2014-supplement.

Hiranuma, N., Augustin-Bauditz, S., Bingemer, H., Budke, C., Curtius, J., Danielczok, A., et al., 2015. A comprehensive laboratory study on the immersion freezing behavior of illite NX particles: a comparison of 17 ice nucleation measurement techniques. Atmos. Chem. Phys. 15 (5), 2489–2518. https://doi.org/10.5194/acp-15-2489-2015-supplement.

Jiang, H., Cotton, W.R., Pinto, J., Curry, J., Weissbluth, M.J., 2000. Cloud resolving simulations of mixed-phase Arctic stratus observed during BASE: Sensitivity to concentration of ice crystals and large-scale heat and moisture advection. J. Atmos. Sci. 57 (13), 2105–2117.

Klein, S.A., Mccoy, R.B., Morrison, H., Ackerman, A.S., Avramov, A., Boer, G.D., et al., 2009. Intercomparison of model simulations of mixed-phase clouds observed during the ARM Mixed-Phase Arctic Cloud Experiment. I: single-layer cloud. Q. J. R. Meteorol. Soc. 135, 979–1002. https://doi.org/10.1002/qj.416.

Klingebiel, M., de Lozar, A., Molleker, S., Weigel, R., Roth, A., Schmidt, L., et al., 2015. Arctic low-level boundary layer clouds: in situ measurements and simulations of mono- and bimodal supercooled droplet size distributions at the top layer of liquid phase clouds. Atmos. Chem. Phys. 15 (2), 617–631. https://doi.org/10.5194/acp-15-617-2015.

Korolev, A., Isaac, G., Hallett, J., 2000. Ice particle habits in stratiform clouds. Q. J. R. Meteorol. Soc. 126 (569), 2873–2902.

Korolev, A.V., Emery, E.F., Strapp, J.W., 2011. Small ice particles in tropospheric clouds: fact or artifact? Airborne icing instrumentation evaluation experiment. Bull. Am. Meteorol. Soc. 92 (8), 967–973.

Ladino Moreno, L.A., Stetzer, O., Lohmann, U., 2013. Contact freezing: a review of experimental studies. Atmos. Chem. Phys. 13 (19), 9745–9769. https://doi.org/10.5194/acp-13-9745-2013.

Lawson, R.P., 2011. Effects of ice particles shattering on optical cloud particle probes. Atmos. Meas. Tech. 4 (1), 1361–1381. https://doi.org/10.5194/amtd-4-939-2011.

Lawson, R.P., Woods, S., Morrison, H., 2015. The microphysics of ice and precipitation development in tropical cumulus clouds. J. Atmos. Sci. 72 (6), 2429–2445. https://doi.org/10.1175/JAS-D-14-0274.1.

Leck, C., Bigg, E.K., 2005. Source and evolution of the marine aerosol—a new perspective. Geophys. Res. Lett. 32 (19), L19803. https://doi.org/10.1029/2005GL023651.

Lowenthal, D.H., Borys, R.D., Cotton, W., Saleeby, S., Cohn, S.A., Brown, W.O.J., 2011. Atmospheric environment. Atmos. Environ. 45 (2), 519–522. https://doi.org/10.1016/j.atmosenv.2010.09.061.

Mason, R.H., Si, M., Chou, C., Irish, V.E., Dickie, R., Elizondo, P., et al., 2016. Size-resolved measurements of ice-nucleating particles at six locations in North America and one in Europe. Atmos. Chem. Phys. 16, 1637–1651. https://doi.org/10.5194/acp-16-1637-2016-supplement.

McFarquhar, G.M., Zhang, G., Poellot, M.R., Kok, G.L., McCoy, R., Tooman, T., et al., 2007. Ice properties of single-layer stratocumulus during the mixed-phase arctic cloud experiment (MPACE): part I observations. J. Geophys. Res. 112, D24201. https://doi.org/10.1029/2007JD008633.

McFarquhar, G.M., Ghan, S., Verlinde, J., Korolev, A., Strapp, J.W., Schmid, B., et al., 2011. Indirect and semi-direct aerosol campaign: the impact of arctic aerosols on clouds. Bull. Am. Meteorol. Soc. 92, 183–201. https://doi.org/10.1175/2010BAMS2935.1.

Mellado, J.P., 2016. Cloud-top entrainment in stratocumulus clouds. Annu. Rev. Fluid Mech. 49 (1), 145–169. https://doi.org/10.1146/annurev-fluid-010816-060231.

Mitchell, D., 1988. Evolution of snow-size spectra in cyclonic storms: Part I: snow growth by vapor deposition and aggregation. J. Atmos. Sci. 45 (22), 3431–3452.

Morrison, H., Pinto, J.O., 2004. A new approach for obtaining advection profiles: application to the SHEBA column. Mon. Weather Rev. 132 (3), 687–702.

Morrison, H., Shupe, M., Pinto, J., Curry, J., 2005. Possible roles of ice nucleation mode and ice nuclei depletion in the extended lifetime of Arctic mixed-phase clouds. Geophys. Res. Lett. 32, L18801.

Morrison, H., Pinto, J., Curry, J., McFarquhar, G.M., 2008. Sensitivity of modeled Arctic mixed-phase stratocumulus to cloud condensation and ice nuclei over regionally varying surface conditions. J. Geophys. Res. 113, D05203.

Morrison, H., Zuidema, P., Ackerman, A.S., Avramov, A., De Boer, G., Fan, J., et al., 2011. Intercomparison of cloud model simulations of Arctic mixed-phase boundary layer clouds observed during SHEBA/FIRE-ACE. J. Adv. Model. Earth Syst. 3, 1–23. https://doi.org/10.1029/2011MS000066.

Ovchinnikov, M., Ackerman, A.S., Avramov, A., Cheng, A., Fan, J., Fridlind, A.M., et al., 2014. Intercomparison of large-eddy simulations of Arctic mixed-phase clouds: importance of ice size distribution assumptions. J. Adv. Model. Earth Syst. 6 (1), 223–248. https://doi.org/10.1002/2013MS000282.

Petters, M.D., Wright, T.P., 2015. Revisiting ice nucleation from precipitation samples. Geophys. Res. Lett. 42, 8758–8766. https://doi.org/10.1002/(ISSN)1944-8007.

Phillips, V.T.J., DeMott, P., Andronache, C., 2008. An empirical parameterization of heterogeneous ice nucleation for multiple chemical species of aerosol. J. Atmos. Sci. 65, 2757–2783.

Pinto, J., 1998. Autumnal mixed-phase cloudy boundary layers in the Arctic. J. Atmos. Sci. 55 (11), 2016–2038.

Prenni, A.J., Demott, P.J., Kreidenweis, S.M., Harrington, J.Y., Avramov, A., Verlinde, J., et al., 2007. Can ice-nucleating aerosols affect Arctic seasonal climate? Bull. Am. Meteorol. Soc. 88 (4), 541–550. https://doi.org/10.1175/BAMS-88-4-541.

Prenni, A.J., Demott, P.J., Rogers, D.C., Kreidenweis, S.M., McFarquhar, G.M., Zhang, G., et al., 2009. Ice nuclei characteristics from M-PACE and their relation to ice formation in clouds. Tellus Ser. B Chem. Phys. Meteorol. 61 (2), 436–448. https://doi.org/10.1111/j.1600-0889.2009.00415.x.

Pruppacher, H.R., Klett, J.D., 1997. Microphysics of Clouds and Precipitation, second ed. Kluwer Academic Publishers, Boston, MA.

Rangno, A., Hobbs, P.V., 2001. Ice particles in stratiform clouds in the Arctic and possible mechanisms for the production of high ice concentrations. J. Geophys. Res. 106 (D14), 15065–15075.

Rogers, D., DeMott, P., Kreidenweis, S., Chen, Y., 2001. A continuous-flow diffusion chamber for airborne measurements of ice nuclei. J. Atmos. Ocean. Technol. 18, 725–741.

Savre, J., Ekman, A., 2015a. A theory based parameterization for heterogeneous ice nucleation and implications for the simulation of ice processes in atmospheric models. J. Geophys. Res. 120, 4937–4961. https://doi.org/10.1002/2014JD023000.

Savre, J., Ekman, A.M.L., 2015b. Large-eddy simulation of three mixed-phase cloud events during ISDAC: conditions for persistent heterogeneous ice formation. J. Geophys. Res. 120 (15), 7699–7725. https://doi.org/10.1002/2014JD023006.

Savre, J., Ekman, A.M.L., Svensson, G., Tjernström, M., 2014. Large-eddy simulations of an Arctic mixed-phase stratiform cloud observed during ISDAC: sensitivity to moisture aloft, surface fluxes and large-scale forcing. Q. J. R. Meteorol. Soc. 141 (689), 1177–1190. https://doi.org/10.1002/qj.2425.

Schwarzenboeck, A., Shcherbakov, V., Lefevre, R., Gayet, J.F., Pointin, Y., Duroure, C., 2009. Indications for stellar-crystal fragmentation in Arctic clouds. Atmos. Res. 92, 220–228.

Shupe, M., Matrosov, S., Uttal, T., 2006. Arctic mixed-phase cloud properties derived from surface-based sensors at SHEBA. J. Atmos. Sci. 63 (2), 697–711.

Solomon, A., Feingold, G., Shupe, M.D., 2015. The role of ice nuclei recycling in the maintenance of cloud ice in Arctic mixed-phase stratocumulus. Atmos. Chem. Phys. 15 (18), 10631–10643. https://doi.org/10.5194/acp-15-10631-2015.

Sullivan, R.C., Miñambres, L., Demott, P.J., Prenni, A.J., Carrico, C.M., Levin, E.J.T., et al., 2010. Chemical processing does not always impair heterogeneous ice nucleation of mineral dust particles. Geophys. Res. Lett. 37(24). https://doi.org/10.1029/2010GL045540.

Vali, G., Snider, J.R., 2015. Time-dependent freezing rate parcel model. Atmos. Chem. Phys. 15 (4), 2071–2079. https://doi.org/10.5194/acp-15-2071-2015.

Vali, G., DeMott, P.J., Möhler, O., Whale, T.F., 2015. Technical note: a proposal for ice nucleation terminology. Atmos. Chem. Phys. 15 (18), 10263–10270. https://doi.org/10.5194/acp-15-10263-2015-corrigendum.

Verlinde, J., Harrington, J., Yannuzzi, V.T., Avramov, A., Greenberg, S., Richardson, S.J., et al., 2007. The mixed-phase arctic cloud experiment. Bull. Am. Meteorol. Soc. 88 (2), 205–221. https://doi.org/10.1175/BAMS-88-2-205.

Vogelmann, A.M., Fridlind, A.M., Toto, T., Endo, S., Lin, W., Wang, J., et al., 2015. RACORO continental boundary layer cloud investigations: 1. case study development and ensemble large-scale forcings. J. Geophys. Res. 120, 5962–5992.

Wang, Y., Liu, X., 2014. Immersion freezing by natural dust based on a soccer ball model with the community atmospheric model version 5: climate effects. Environ. Res. Lett. 9(12). https://doi.org/10.1088/1748-9326/9/12/124020.

Westbrook, C.D., Illingworth, A.J., 2013. The formation of ice in a long-lived supercooled layer cloud. Q. J. R. Meteorol. Soc. 139 (677), 2209–2221. https://doi.org/10.1002/qj.2096.

Wright, T.P., Petters, M.D., Hader, J.D., Morton, T., Holder, A.L., 2013. Minimal cooling rate dependence of ice nuclei activity in the immersion mode. J. Geophys. Res. 118 (18), 10535–10543. https://doi.org/10.1002/jgrd.50810.

Yang, F., Ovchinnikov, M., Shaw, R.A., 2013. Minimalist model of ice microphysics in mixed-phase stratiform clouds. Geophys. Res. Lett. 40 (14), 3756–3760. https://doi.org/10.1002/grl.50700.

Yang, F., Ovchinnikov, M., Shaw, R.A., 2014. Microphysical consequences of the spatial distribution of ice nucleation in mixedphase stratiform clouds. Geophys. Res. Lett. 41, 5280–5287. https://doi.org/10.1002/2014GL060657.

Yano, J.-I., Phillips, V.T.J., 2011. Ice–ice collisions: an ice multiplication process in atmospheric clouds. J. Atmos. Sci. 68 (2), 322–333. https://doi.org/10.1175/2010JAS3607.1.

Zuidema, P., Baker, B., Han, Y., Intrieri, J., Key, J., Lawson, P., et al., 2005. An Arctic springtime mixed-phase cloudy boundary layer observed during SHEBA. J. Atmos. Sci. 62 (1), 160–176.